

Analog-antianalog isospin mixing in ^{47}K β^- decay

Brian Kootte¹, H. Gallop^{1,3}, C. Luktuke^{1,3}, J.C. McNeil^{3,1}, A. Gorelov¹,

D. Melconian^{4,5}, J. Klimo^{4,5}, B.Vargas-Calderon^{4,5}, and J.A. Behr^{1,2*}

¹TRIUMF, 4004 Wesbrook Mall, Vancouver, BC V6T 2A3 Canada

²University of British Columbia, Department of Physics and Astronomy,
6224 Agricultural Road, Vancouver, B.C. V6T 1Z1 Canada

³University of Waterloo, Department of Physics and Astronomy,
200 University Ave W, Waterloo, ON N2L 3G1

⁴Cyclotron Institute, Texas A&M University, 3366 TAMU, College Station, Texas 77843-3366, USA

⁵Department of Physics and Astronomy, Texas A&M University,
4242 TAMU, College Station, Texas 77843-4242, USA

(Dated: February 28, 2024)

We have measured the isospin mixing of the $I^\pi = 1/2^+$ $E_x = 2.599$ MeV state in nearly-doubly-magic ^{47}Ca with the isobaric analog $1/2^+$ state of ^{47}K . Using the TRIUMF atom trap for β decay, we have measured a nonzero asymmetry of the progeny ^{47}Ca with respect to the initial ^{47}K spin polarization, which together with the β asymmetry implies a nonzero ratio of Fermi to Gamow-Teller matrix elements $y = 0.098 \pm 0.037$. Interpretation as mixing between this state and the isobaric analog state implies a Coulomb matrix element magnitude 101 ± 37 keV. This relatively large matrix element supports a model from the literature of analog-antianalog isospin mixing, which predicts large matrix elements in cases involving excess neutrons over protons occupying more than one major shell. The result supports pursuing a search for time-reversal odd, parity-even, isovector interactions using a correlation in ^{47}K β decay.

I. INTRODUCTION

The neutron beta decays to its isobaric analog state, the proton, as does tritium. Many other isotopes undergo beta minus decay to states of same spin I and parity π , but because of the extra Coulomb energy at higher Z , decay to the isobaric analog state is energetically forbidden. So the Gamow-Teller operator dominates, while the Fermi operator linking isobaric analog states is only allowed if some low-lying final state of same I^π is mixed by an isospin-breaking interaction with the excited isobaric analog. We see such isospin breaking in an $I^\pi = 1/2^+$ state in the ^{47}Ca nucleus 80% fed by the beta decay of ^{47}K . Interference between Gamow-Teller and isospin-suppressed Fermi amplitudes produces an asymmetry of the progeny recoil direction with respect to the initial nuclear spin, which we measure with TRIUMF's Neutral Atom Trap for β decay (TRINAT).

Since ^{47}Ca and ^{47}K are near closed shells, the single known ^{47}Ca $1/2^+$ state may contain much of the antianalog configuration, and is predicted to have a relatively large Coulomb mixing matrix element with the analog [1]. Sensitivity to time reversal-odd parity-even (TOPE) inherently isovector [2] N-N interactions through a β - ν -spin correlation is thought to be enhanced in these systems, as the small amount of time reversal is referenced to Coulomb rather than strong interactions [3], which motivates our measurement of isospin breaking in ^{47}K decay.

II. THEORY AND METHODS

A. Analog \mathcal{A} - antianalog $\bar{\mathcal{A}}$ mixing

The antianalog configuration has same spin and occupancy of spatial orbitals as the isobaric analog, but has total isospin reduced to $T = T_z$, with the antisymmetry of its wavefunction encoded differently between spin and isospin parts so that it is orthogonal to the analog state. Auerbach and Loc [1], using schematic wavefunctions, write a closed-form expression for analog-antianalog Coulomb mixing for n_1 and n_2 excess neutrons over protons occupying orbitals j_1 and j_2 :

$$H_C = \langle \bar{\mathcal{A}} | V_C | \mathcal{A} \rangle = \frac{\sqrt{n_1 n_2}}{2T} (\langle j_1 | V_C | j_1 \rangle - \langle j_2 | H_C | j_2 \rangle) \quad (1)$$

$$\rightarrow 0.35 \frac{\sqrt{n_1 n_2}}{2T} \frac{Z}{A^{2/3}} \text{MeV}, \quad (2)$$

for harmonic oscillator wavefunctions, a uniform charge distribution, and cases where neutrons occupy two major shells differing by one $\hbar\omega$. Ref. [1], using experimental Coulomb energies from mirror nuclei, note that Eq. 1 produces for occupancy of both the $p_{3/2}$ or $p_{5/2}$ and $f_{5/2}$ or $f_{7/2}$ subshells H_C about a factor of two smaller than the major shell-occupancy Eq. 2, thus $f_{7/2}$ is not a major shell when considering Coulomb energies. Ref [1] then benchmark these simple expressions with RPA calculations to an accuracy of $\sim 20\%$. Eq. 2 predicts $H_C = 160$ keV for our case $^{47}\text{K}^{28}$ (with $n_1 = 8$ $f_{7/2}$ neutrons and $n_2 = 1$ $2s_{1/2}$ neutron).

* behr@triumf.ca

B. Isospin-suppressed β decay

In the angular distribution for allowed $I=1/2$ β decay in terms of lepton momentum p and energy E [4]:

$$dW = F(E, Z)pE p_\nu E_\nu \left(1 + a \frac{\vec{p}_\beta \cdot \vec{p}_\nu}{E_\beta E_\nu} + \hat{I} \cdot (A_\beta \frac{\vec{p}_\beta}{E_\beta} + B_\nu \frac{\vec{p}_\nu}{E_\nu})\right), \quad (3)$$

isospin-suppressed Fermi decay alters the correlation coefficients from their Gamow-Teller values:

$$a = \frac{y^2 - 1/3}{y^2 + 1}; A_\beta = A_{\beta GT} + f(M_F); B_\nu = -A_{\beta GT} + f(M_F) \quad (4)$$

with $y = g_V M_f / g_A M_{GT}$ and $f(M_F) = 2\sqrt{\frac{J}{J+1}} \frac{y}{1+y^2}$. The recoil asymmetry is then proportional to $A_\beta + B_\nu$, which vanishes when $M_F=0$. (Analytic expressions for the proportion, which are possible if the Fermi function is set to unity, are given in Refs. [5, 6]: we compare here entirely to numerical simulations.)

C. ^{47}K and its β^- decay to ^{47}Ca

The ^{47}K $I^\pi=1/2^+$ ground-state has magnetic moment $1.933(9) \mu_N$ [7], close enough to the proton μ to suggest a large fractional component of single-particle $2s_{1/2}$. The 80% β^- branch to the $1/2^+$ 2.599 MeV state (Fig. 1) has $\log(ft)=4.81$, for which a literature shell-model calculation of the Gamow-Teller strength finds $\log(ft)_{GT} = 4.39$ [8]. This experimental $g_A |M_{GT}| = 0.305$ is considerably smaller than the single-particle $2s_{1/2}$ GT value of $\sqrt{3}$. We include in our simulations the $18.4 \pm 0.3\%$ branch to the 2.578 MeV first excited $3/2^+$ state, and another 1.3% known to decay to five other $3/2^+$ states [9]: these can have no Fermi component and so simply dilute our measured A_{recoil} . For pure Gamow-Teller decay, the beta asymmetry $A_{\beta GT} = -2/3$ for the $1/2^+ \rightarrow 1/2^+$ transition and $+1/3$ for the $1/2^+ \rightarrow 3/2^+$ transitions, so the precision of their weighted average $A_{\beta GT} = -0.467 \pm 0.020$ is needed to extract M_F from A_β .

Ref. [9] also observes 0.042% to first-forbidden branches— although these can have asymmetries near unity, we can safely ignore them at our achieved accuracy. The experimental upper limit for direct β decay to the 2.013 MeV first $3/2^-$ state would increase our uncertainty from branching ratios in Table I by a factor of 1.5. We constrain this branch with a calculation of the first-forbidden nonunique fT value [8] of 0.25%; our assignment of 0.25% uncertainty does not perturb our uncertainty.

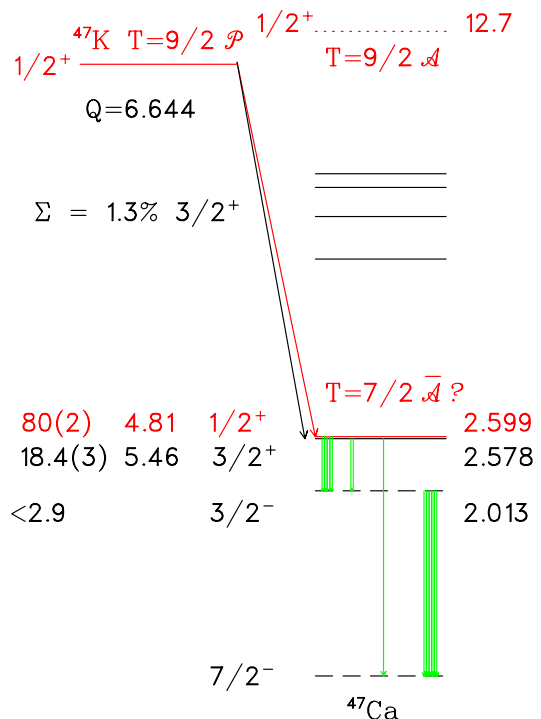


FIG. 1. Relevant allowed decay of ^{47}K , showing β^- branches $>0.04\%$, $\log(ft)$, I^π , energy [MeV], and isospin T of the isobaric parent \mathcal{P} , analog \mathcal{A} , and possible antianalog $\bar{\mathcal{A}}$. Thickness of γ transitions $>5\%$ indicate intensity.

III. EXPERIMENT:

A. TRIUMF Neutral Atom Trap

Fig. 2 is a side view of the detection apparatus of TRIUMF's Neutral Atom Trap for β decay (TRINAT). Not shown is the collection trap from a vapour cell cube nor the push beams [10].

Using $6 \times 10^6/\text{s}$ mass-separated ^{47}K delivered from the TRIUMF/ISAC isotope separator on-line facility, we trapped on average 500-1,000 ^{47}K atoms during the data-taking time. We optimized the number of atoms when the trapping light was tuned about 3 linewidths to the red of the $4S_{1/2}$ to $4P_{3/2}$ $F=1$ to $F=2$ transition, as measured with respect to the optical resonance measured by Ref. [7]. Repumping light on the $F=0$ to $F=1$ transition was provided by 3.3 GHz fiber-coupled electro-optic modulators.

B. Polarization by optical pumping

Details of optical pumping are very similar to our ^{37}K measurement [11]. Changes include much thinner pelli-cle mirrors along the optical pumping axis to reduce β straggling, made from 4 micron thick polyimide coated with 100 nm of Au. The optical pumping light quality is improved from 0.991 to closer to 0.995 Stokes S_3 .

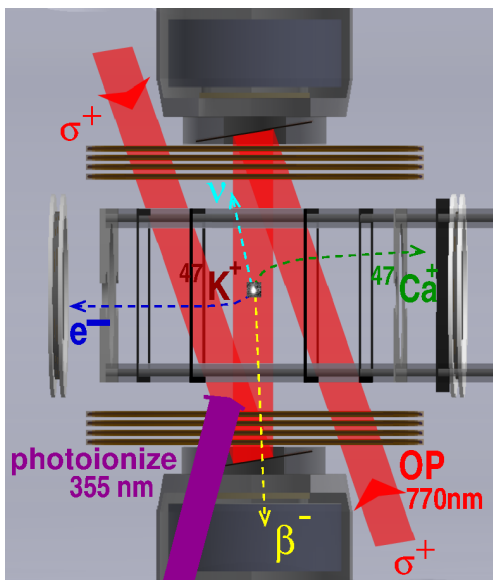


FIG. 2. TRINAT during the optical pumping time. Shown are β telescopes, mirrors for optical pumping light and its beams, magnetic field coils, electric field electrodes, and microchannel plates for electron and ion detection. A CMOS camera image of 1,000 trapped atoms is superimposed. Distance between trap cloud and ion MCP is 9.7 cm.

We alternate 2.9 ms trapping with 1.1 ms optical pumping, during which we make the polarized beta decay measurements. During the polarization time, we switch the magnetic field from the trap's quadrupole to a uniform 1 Gauss field pointed up, and apply circularly polarized light along the quantization axis. Once we start the OP cycle, atoms increase spin to maximum, then stop absorbing in the $S_{1/2}$ to $P_{1/2}$ transition used. If instead the light is linearly polarized, atoms keep absorbing, and the atoms and nuclei remain unpolarized.

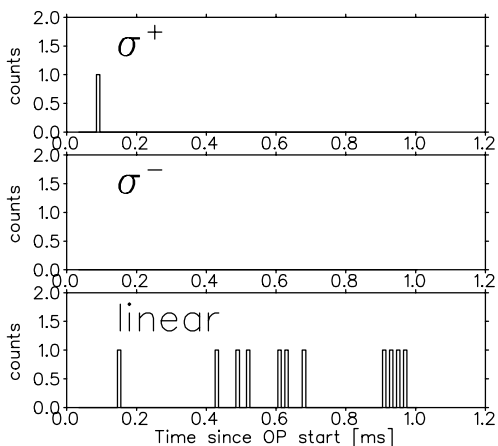


FIG. 3. Excited state population during the optical pumping time for circularly and linearly polarized light. See text for deduction of nuclear polarization.

Once excited, 0.5 nsec pulsed light with rep rate 10

KHz from a 355 nm laser has enough energy/photon to photoionize about $1/10^6$ atoms per pulse, detected in the same ion microchannel-plate detector (MCP) used for the ^{47}Ca recoils from β decay. The photoions are distinguished by their time-of-Flight (TOF) and by their centre position, and we use them to determine average trap cloud sizes and positions when the MOT light is on.

The vanishing of photoion rate during the polarization time is then our probe of the atomic polarization quality. In Fig. 3 we show 11 photoions while linearly polarized (in about 1/4 the total time measured) and 1 photon circularly polarized. For spin-1/2 all the sub-level transitions have equal probabilities, making the deduced nuclear polarization simple to deduce, nearly independent of which nearly fully polarized states are excited. We deduce a fraction of nuclear polarization achieved for the decaying ^{47}K atoms of $P = \langle I_z \rangle / I = 0.96 \pm 0.04$. We find the polarization extracted by rate equations from this circular/linear ratio is independent of power and detuning of the optical pumping light to well within this accuracy.

C. Geometry and Detectors

An electric field is formed by a combination of low-Z glassy carbon and titanium electrodes to minimize β scattering. The field is calculated by standard finite element techniques to have average 650 V/cm, and after comparing with a full simulation tracing trajectories in the detailed field, we found that taking this average as a uniform field is sufficiently accurate for our asymmetry simulations. The field collects ^{47}Ca ions produced in ^{47}K β^- decay to an MCP with 78 mm active diameter located 9.7 cm away. Decay by β^- naturally makes $^{47}\text{Ca}^{+1}$ ions. Additional low-energy atomic shakeoff electrons, which take an average of 6 ns to reach the opposite 40 mm diameter MCP, provide a starting trigger for the TOF of $^{47}\text{Ca}^{+2}$ and higher.

Critical to β detection is discriminating β 's from γ 's, because their ratio in ^{47}K decay is about 1 to 2. We use the same 0.30 mm thick double-sided silicon strip detectors as Ref. [12], similarly requiring both X and Y strips above energy threshold and similar calibrated energy deposited. Our plastic 4x9cm scintillators for β^+ detection now use Silicon Photomultiplier (SiPM) readouts and are characterized in Ref. [13].

IV. RESULTS

A. e^- -Recoil ^{47}Ca Ion Coincidences

Our main channel is coincidences between decay recoils on the ion MCP and shakeoff electrons on the e^- MCP. The TOF spectrum in Fig. 4 has contributions from ^{47}Ca charge states +2 through +7. Their position asymmetry along the polarization axis is shown to be nonzero in Fig. 5, directly implying a nonzero Fermi contribution to

the $1/2^+ \rightarrow 1/2^+$ transition. (Since β^- decay makes +1 ions without shakeoff, these are from β^- 's and γ 's firing the electron MCP and accidentals, so we do not use them for A_{recoil} .)

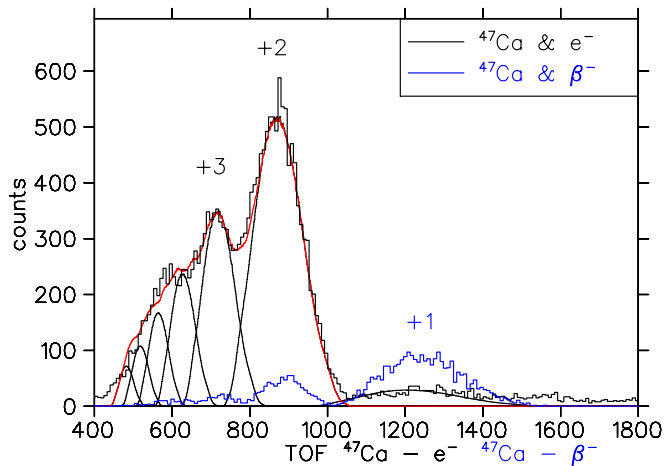


FIG. 4. Time-of-Flight (TOF) of ^{47}Ca +2 to +7 ions started by shakeoff e^- , showing the modelled data decomposition. Blue histogram: TOF started by β^- 's in the $\Delta E - E$ telescopes, which have lower statistics but less background from untrapped atoms and accidentals.

We model this by a numerical integration of β and ν (Eqs. 1-2), with the resulting ^{47}Ca ions collected to the ion MCP by the uniform 650 V/cm electric field. We find it adequate to include the momentum perturbation on the ^{47}Ca from a single 2 MeV γ subsequently emitted isotropically — note emission of the dominant γ in Fig. 1 must be isotropic. The result is $y = +0.103 \pm 0.041$ (a solution with $y \sim 10$ is physically excluded). Systematic uncertainties are listed in Table I.

TABLE I. Systematic uncertainties. Both observables are statistics dominated. NA denotes not applicable. Listed common systematics are so different between observables that we are not concerned with their correlation.

Source	A_{recoil}	pseudo A_β
A_{recoil} bkg $6 \pm 4\%$	0.014	< 0.002
Polarization 0.96 ± 0.04	0.004	0.023
β^- Branching ratio	0.002	0.022
Weak magnetism	0.0006	0.0003
Fit range in $Z \pm 20$ to 34 mm	0.012	NA
$^{47}\text{Ca}^{+1}$ percent bkg	0.001	NA
$^{47}\text{Ca}^{+N}$ distribution from TOF	< 0.0005	NA
E field	negligible	0.025
Backscatter correction $-0.012 \pm 20\%$	NA	0.0024
Fit statistics	0.037	0.082
Total	0.041	0.091

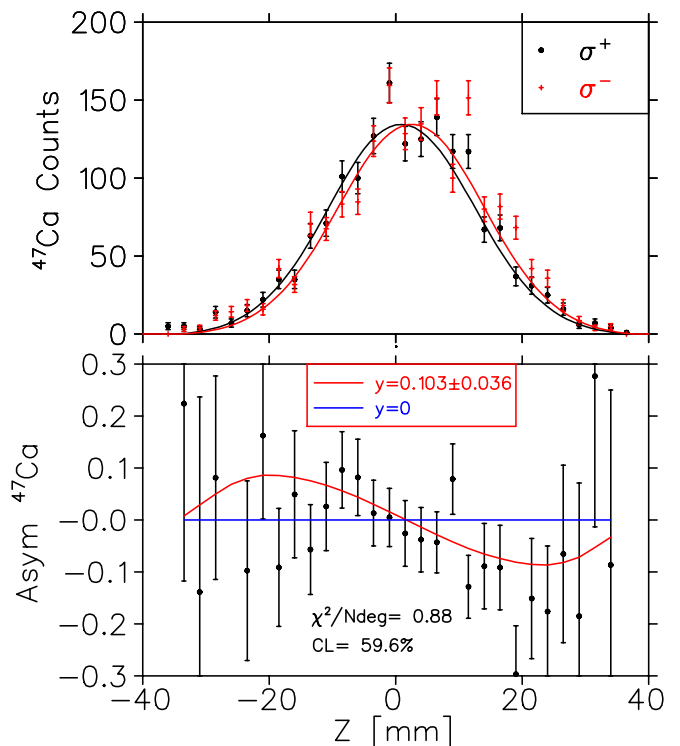


FIG. 5. Top: Distribution along polarization axis Z of $^{47}\text{Ca}^{+2\dots7}$ in coincidence with shakeoff e^- 's, for the two polarizations. Bottom: The asymmetry of these distributions, i.e. the difference divided by the sum of the Top distributions. The nonzero asymmetry scales with y , and directly implies a nonzero Fermi contribution.

1. Backgrounds from untrapped atoms

The vacuum-limited trap half-life of 10 sec and the $t_{1/2}=17.5$ sec of ^{47}K implies that more than half the nuclei decay after the atoms leave the trap. We have measured this background with 1 hour of data while deliberately ejecting atoms from the trap. We deduce a background of $6 \pm 4\%$ of the events in the $e^- - ^{47}\text{K}$ channel, roughly flat in TOF in the region we use of +2 through +7 charge states, and include that background in our simulation. This is consistent with a small fraction of the untrapped atoms sticking to the glassy carbon electrodes close to the trap, while shakeoff electrons from other surfaces are excluded from the electron MCP by the electric field. Our β collimation is sufficient that we see backgrounds consistent with zero for the β -recoil channel considered below.

B. β -Recoil Coincidences Using Pseudo A_β

We also measure β^- 's in coincidence with ^{47}Ca recoils. If we measured ^{47}Ca recoils over all directions and momenta, this would be a measurement of A_β . However, some $^{47}\text{Ca}^{+1}$ ions with high transverse momenta do not

impact the MCP, perturbing the asymmetry of β 's in coincidence by a well-defined combination of the β - ν correlation and the ν asymmetry.

This observable, which we name $\text{pseudo}A_\beta$, we also model by numerical integration, including the effects of a single 2 MeV γ . We group the four combinations of β detector and polarization sign in pairs to cancel asymmetries. The results are in Fig. 6, where the different counting times of the 2 polarization states are included in the simulation. Numerical simulations for three values of M_F/M_{GT} show sensitivity to the asymmetry, along with the best fit. A single straight line for $M_F=0$ and hypothetical full collection of ^{47}Ca is shown to indicate how the asymmetries are distorted from A_β . The significantly smaller difference in asymmetry for positive vs. negative Z is due to 0.22 and 0.45 mm displacements in the cloud Z and horizontal position and subsequent change in ^{47}Ca collection, and is well-reproduced by the simulation.

We note that the sign of A_β is determined from this observable. We use this to determine the sign of our spin polarization.

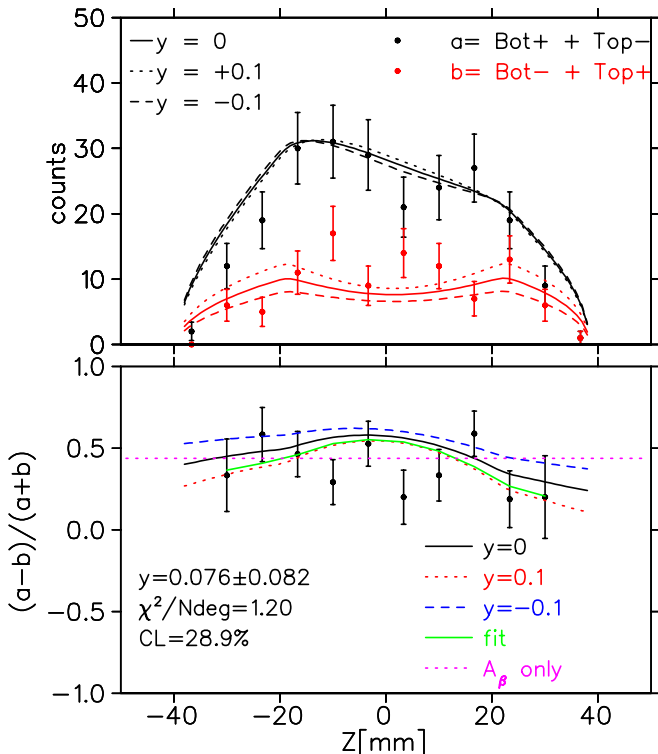


FIG. 6. Similar to Fig. 5, but for β - $^{47}\text{Ca}^{+1}$ coincidences.

To deduce a Fermi contribution from $\text{pseudo}A_\beta$ requires more precision and accuracy than A_{recoil} , because we must distinguish between the experimental value and the nonzero theoretical value of $A_\beta = -0.467$ assuming pure Gamow-Teller transitions. The uncertainties are summarized in Table I. Based on our previous ^{37}K A_β measurement [12], we scale our experimental value by $1/1.023$ to approximately account for backscatter, assigning here a more generous uncertainty of 20% because we

have not done full simulations of geometry changes.

The result from $\text{pseudo}A_\beta$, $y=0.076\pm 0.091$, is consistent in sign with A_{recoil} , but with larger uncertainty.

1. Recoil order corrections.

We use Ref. [14, 15] for the correction from the recoil kinetic energy, the 1st-order in recoil correction from weak magnetism b_W , and the Coulomb finite-size correlation correction. Assuming the wavefunction of initial and final $1/2^+$ states is an $s_{1/2}$ nucleon, b_W has no orbital angular momentum contribution and becomes the nucleon value [16]: the first-class induced tensor d_I also vanishes for $s_{1/2}$. Similarly assuming single-particle $s_{1/2} \rightarrow d_{3/2}$ for the 20% branches to $3/2^+$ states, the orbital correction to b is zero if l changes; here we ignore potentially nonzero d_I and 2nd-order in recoil corrections because of the 20% fraction. The recoil corrections increase our deduced A_{recoil} by 0.0025, 0.0012 from b_W to which we assign 50% uncertainty; the Coulomb finite-size correction decreases A_{recoil} by 0.0017. Similarly, b_W changes $\text{pseudo}A_\beta$ by 0.0006 ± 0.0003 .

C. Result and Isospin breaking

Our weighted average of results from A_{recoil} and $\text{pseudo}A_\beta$ is then $y = g_V M_F / g_A M_{GT} = 0.098\pm 0.037$ for the $1/2^+$ to $1/2^+$ transition.

Given the measured $g_A M_{GT} = 0.305$, we deduce $|M_F| = 0.030\pm 0.011$ (assuming the standard model value of $g_V = 1.00$, and that we do not know the sign of M_{GT}). To compare to other nuclei thought to be dominated by $\mathcal{A} - \bar{\mathcal{A}}$ mixing, we use a first-order perturbation theory expression from the literature, including the standard ladder operator result for isospin [21, 24]: $M_F = \frac{\langle \mathcal{A} | H_C | \bar{\mathcal{A}} \rangle}{\Delta E} \sqrt{(T \mp T_z)(T \pm T_z + 1)}$ (upper vs. lower sign for β^- vs. β^+), along with the measured $\bar{\mathcal{A}} - \mathcal{A}$ splitting $\Delta E = 10.1$ MeV [25], to deduce a Coulomb matrix element $|H_C| = 101 \pm 37$ keV.

This Coulomb matrix element is over half of the 160 keV prediction of $\mathcal{A} - \bar{\mathcal{A}}$ mixing. We attribute this to the simple structure of nearly-doubly magic ^{47}Ca and its single $1/2^+$ state. That this is not the full prediction suggests the state is somewhat more complex than $\bar{\mathcal{A}}$.

Many β decays in such systems have much smaller Coulomb matrix elements and M_F . Ref. [1] suggests the $\bar{\mathcal{A}}$ configuration is often fragmented among many states. Fig. 7, a plot of literature measurements of y [21], suggests that M_F can maintain a substantial fraction of M_{GT} even as $|M_{GT}|$ decreases by two orders of magnitude, suggesting general decrease of both with the complexity of nuclear states. Fig 7 also shows $|H_C|$ with estimates from $\mathcal{A} - \bar{\mathcal{A}}$ mixing. There are several cases with neutron excess in both 2p and 1f orbitals with relatively large M_F and H_C , factors of 2-4 smaller than their similar

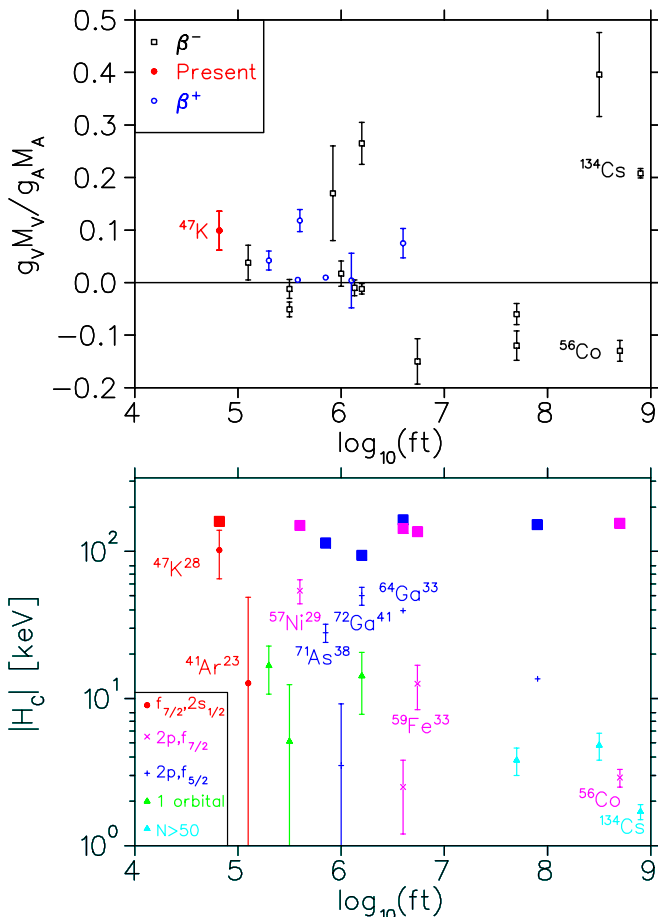


FIG. 7. y as a function of $\log(ft)$ for isospin-suppressed transitions (Refs. [17–23]). Bottom: Deduced H_C from isospin-forbidden β decay experiments. Solid squares show calculation of $\mathcal{A} - \bar{\mathcal{A}}$ mixing from Eqs. 1 and 2 [1].

H_C predictions from Eq. 1 [1]. In contrast, the β^+ decay of ^{56}Co has a strikingly small H_C , given its relevant isobaric parent \mathcal{P} ^{56}Fe also has excess neutrons spanning the $N=28$ shell closure: one explanation would be fragmentation of the $\bar{\mathcal{A}}$ configuration. Cases with excess neutrons all in one orbital tend to have smaller H_C , consistent with little $\mathcal{A} - \bar{\mathcal{A}}$ mixing, though the most striking trend is the general drop of $|H_C|$ with GT strength.

Ref. [3] proposes a time-reversal measurement in ^{134}Cs , which has a very slow M_{GT} transition and small Coulomb matrix element. A measurement was similarly pursued in ^{56}Co [26]. For isovector TOPE nucleon-nucleon [27] matrix elements having similar dependence on nuclear complexity (e.g. a long-ranged isovector Yukawa could be similar to Coulomb), a faster decay like ^{47}K with its large $\bar{\mathcal{A}}$ component and its sizable y could also be a favourable system for a time-reversal search.

V. CONCLUSION

For the ^{47}K β^- $1/2^+ \rightarrow 1/2^+$ transition, we have measured the ratio of Fermi to Gamow-Teller matrix elements $y=0.098 \pm 0.037$, and from the known GT strength we deduce $|M_F|=0.030 \pm 0.011$ Interpreted as $\mathcal{A} - \bar{\mathcal{A}}$ mixing in the progeny ^{47}Ca , this result implies a relatively large effective Coulomb mixing matrix element magnitude 101 ± 37 keV. A large matrix element of 160 keV is generated for ^{47}Ca from $\mathcal{A} - \bar{\mathcal{A}}$ mixing, as its excess neutrons over protons occupy two major shells, $f_{7/2}$ and sd , with naturally different Coulomb energies [1]. The large fraction observed of that prediction we attribute to the existence of only one $1/2^+$ state in the nearly-doubly-magic ^{47}Ca .

- [1] N. Auerbach and M. L. Bui, Coulomb corrections to fermi beta decay in nuclei, *Nuclear Physics A* **1027**, 122521 (2022).
- [2] M. Simoni, Constraints on parity-even time reversal violation in the nucleon-nucleon system and its connection to charge symmetry breaking, *Phys. Rev. Lett.* **78**, 4161 (1997).
- [3] A. Barroso and R. Blin-Stoyle, A test for time-reversal violation in allowed isospin-hindered beta-decay, *Physics Letters B* **45**, 178 (1973).
- [4] J. Jackson, S. Treiman, and H. Wyld, Coulomb corrections in allowed beta transitions, *Nuclear Physics* **4**, 206 (1957).
- [5] J. R. A. Pitcairn, D. Roberge, A. Gorelov, D. Ashery, O. Aviv, J. A. Behr, P. G. Bricault, M. Dombisky, J. D. Holt, K. P. Jackson, B. Lee, M. R. Pearson, A. Gaudin, B. Dej, C. Höhr, G. Gwinner, and D. Melconian, Tensor interaction constraints from β -decay recoil spin asymmetry of trapped atoms, *Phys. Rev. C* **79**, 015501 (2009).
- [6] S. B. Treiman, Recoil effects in k capture and β decay, *Phys. Rev.* **110**, 448 (1958).
- [7] F. Touchard, P. Guimbal, S. Büttgenbach, R. Klapisch, M. De Saint Simon, J. Serre, C. Thibault, H. Duong, P. Juncar, S. Liberman, J. Pinard, and J. Vialle, Isotope shifts and hyperfine structure of 38–47k by laser spectroscopy, *Physics Letters B* **108**, 169 (1982).
- [8] P. Choudhary, A. Kumar, P. C. Srivastava, and T. Suzuki, Structure of $^{46,47}\text{Ca}$ from the β^- decay of $^{46,47}\text{K}$ in the framework of the nuclear shell model, *Phys. Rev. C* **103**, 064325 (2021).
- [9] J. K. Smith, A. B. Garnsworthy, J. L. Pore, C. Andreoiu, A. D. MacLean, A. Chester, Z. Beadle, G. C. Ball, P. C. Bender, V. Bildstein, R. Braid, A. D. Varela, R. Dunlop, L. J. Evitts, P. E. Garrett, G. Hackman, S. V. Ilyushkin, B. Jigmeddorj, K. Kuhn, A. T. Laffoley, K. G. Leach, D. Miller, W. J. Mills, W. Moore, M. Moukadam, B. Olaizola, E. E. Peters, A. J. Radich, E. T. Rand, F. Sarazin, C. E. Svensson, S. J. Williams, and S. W. Yates, Spectroscopic study of ^{47}Ca from the β^- decay of ^{47}K , *Phys. Rev. C* **102**, 054314 (2020).
- [10] T. B. Swanson, D. Asgeirsson, J. A. Behr, A. Gorelov, and D. Melconian, Efficient transfer in a double magneto-

- optical trap system, *J. Opt. Soc. Am. B* **15**, 2641 (1998).
- [11] B. Fenker, J. A. Behr, D. Melconian, R. M. A. Anderson, M. Anholm, D. Ashery, R. S. Behling, I. Cohen, I. Craiciu, J. M. Donohue, C. Farfan, D. Friesen, A. Gorelov, J. McNeil, M. Mehlman, H. Norton, K. Olchanski, S. Smale, O. Thériault, A. N. Vantygghem, and C. L. Warner, Precision measurement of the nuclear polarization in laser-cooled, optically pumped ^{37}K , *New Journal of Physics* **18**, 073028 (2016).
- [12] B. Fenker, A. Gorelov, D. Melconian, J. A. Behr, M. Anholm, D. Ashery, R. S. Behling, I. Cohen, I. Craiciu, G. Gwinner, J. McNeil, M. Mehlman, K. Olchanski, P. D. Shidling, S. Smale, and C. L. Warner, Precision measurement of the β asymmetry in spin-polarized ^{37}K decay, *Phys. Rev. Lett.* **120**, 062502 (2018).
- [13] M. Ozen, J. A. Behr, M. Khoo, F. Klose, A. Gorelov, and D. Melconian, Lineshape response of plastic scintillator to pair production of 4.44 meV γ 's, *Nuclear Instruments and Methods in Physics Research Section A: Accelerators, Spectrometers, Detectors and Associated Equipment* **1055**, 168490 (2023).
- [14] B. R. Holstein, Recoil effects in allowed beta decay: The elementary particle approach, *Rev. Mod. Phys.* **46**, 789 (1974).
- [15] B. R. Holstein, Erratum: Recoil effects in allowed beta decay: The elementary particle approach, *Rev. Mod. Phys.* **48**, 673 (1976).
- [16] X. B. Wang and A. C. Hayes, Weak magnetism correction to allowed β decay for reactor antineutrino spectra, *Phys. Rev. C* **95**, 064313 (2017).
- [17] L. G. Mann, D. C. Camp, J. A. Miskel, and R. J. Nagle, New measurements of β -circularly-polarized γ angular-correlation asymmetry parameters in allowed β decay, *Phys. Rev.* **139**, AB2 (1965).
- [18] J. Atkinson, L. Mann, K. Tirsell, and S. Bloom, Coulomb matrix elements from β - γ (cp) correlation measurements in ^{57}Ni and ^{65}Ni , *Nuclear Physics A* **114**, 143 (1968).
- [19] H. Behrens, Messung des asymmetrie-koeffizienten der β - γ -zirkularpolarisationskorrelation an erlaubten β -übergängen, *Z. Physik* **201**, 153 (1967).
- [20] J. Markey and F. Boehm, Fermi—gamow-teller interference in ^{56}Co decay, *Phys. Rev. C* **26**, 287 (1982).
- [21] S. Bhattacharjee, S. Mitra, and H. Padhi, Fermi matrix elements in allowed beta transitions in ^{56}Co , ^{58}Co and ^{134}Cs , *Nuclear Physics A* **96**, 81 (1967).
- [22] N. Severijns, D. Vénos, P. Schuurmans, T. Phalet, M. Hounsek, D. Srnka, B. Vereecke, S. Versyck, D. Zákoucký, U. Köster, M. Beck, B. Delauré, V. Golovko, and I. Kraev, Isospin mixing in the $t = 5/2$ ground state of ^{71}As , *Phys. Rev. C* **71**, 064310 (2005).
- [23] P. Schuurmans, J. Camps, T. Phalet, N. Severijns, B. Vereecke, and S. Versyck, Isospin mixing in the ground state of ^{52}Mn , *Nuclear Physics A* **672**, 89 (2000).
- [24] S. D. Bloom, Isotopic-spin conservation in allowed β -transitions and coulomb matrix elements, *Il Nuovo Cimento* **32**, 1023 (1964).
- [25] T. Burrows, Nuclear data sheets for $a = 47$, *Nuclear Data Sheets* **108**, 923 (2007).
- [26] F. P. Calaprice, S. J. Freedman, B. Osgood, and W. C. Thomlinson, Test of time-reversal invariance in the beta decay of ^{56}Co , *Phys. Rev. C* **15**, 381 (1977).
- [27] P. Herczeg, The general form of the time-reversal non-invariant internucleon potential, *Nuclear Physics* **75**, 655 (1966).